

Biexcitonic resonance in the nonlinear optical response of an InAs quantum dot ensemble

A. S. Lenihan,* M. V. Gurudev Dutt, and D. G. Steel†

*The FOCUS Center, H. M. Randall Laboratory of Physics, and The Center for Ultrafast Optical Science,
The University of Michigan, Ann Arbor, Michigan 48109, USA*

S. Ghosh and P. Bhattacharya

*The Solid-State Electronics Laboratory, Department of Electrical Engineering and Computer Science,
The University of Michigan, Ann Arbor, Michigan 48109, USA*

(Received 21 May 2003; published 9 January 2004)

Transient spectral hole burning measurements are applied to an ensemble of InAs self-assembled quantum dots. In addition to the expected exciton hole, we observe an “antihole” due to an induced absorption corresponding to the biexciton state. The biexciton binding energy is consistent with previous measurements in similar systems. The variation of the binding energy over the inhomogeneous quantum dot distribution is also measured, and is found to be consistent with expectations for strongly confined systems as a function of confinement.

DOI: 10.1103/PhysRevB.69.045306

PACS number(s): 78.67.Hc, 71.35.-y, 81.07.Ta

Recently, significant research effort has been applied towards improving the understanding of optically created excitons in semiconductor quantum dots. One motivation for the investigation has been the proposed implementation of these systems in the construction of quantum logic gates.^{1,2} These proposals have been bolstered by recent experimental results, which have demonstrated Rabi flopping,^{3–6} nonradiative coherence and entanglement of exciton polarization states,^{7,8} and extremely long excitonic dephasing times in some of these systems.^{9,10} These studies have focused on the response of single exciton states. However, it is also important for both the complete understanding of quantum dots and their application to quantum computing to study the excitonic molecule, or biexciton, formed by two interacting excitons. Single quantum dot photoluminescence (PL) measurements have allowed for the observation of biexciton resonances in a number of material systems,^{11–14} including $\text{In}_x\text{Ga}_{1-x}\text{As}$ -based self-assembled quantum dots.^{15–17} However, the use of nonlinear techniques to study the biexcitonic response in these systems offers significant advantages, such as their sensitivity to quantum coherences,¹⁸ a necessary requirement for quantum logic operations.

In this paper, we report on nondegenerate differential transmission (DT) measurements performed in an ensemble of InAs/GaAs self-assembled quantum dots. In this case, a standard pump and probe geometry¹⁹ is used, but the pump and probe pulses have independently controllable center frequencies. Previously, nondegenerate DT techniques have been used to investigate applications such as quantum dot hole burning memories,^{20,21} and relaxation between different energy levels of the quantum dot system.^{22–24} Here, however, we examine the nonlinear response resulting from the biexciton state of the quantum dots. The data is found to agree with the modified polarization selection rules which result from the structural asymmetry of the quantum dots. In addition, we study the dependence of the biexciton binding energy on the size of the quantum dot, observing behavior which is consistent with the strongly-confined nature of these dots.

I. SAMPLE CHARACTERISTICS

A sample consisting of a single layer of InAs quantum dots grown on GaAs was used in these measurements. The structure was prepared via molecular-beam epitaxy in the Stranski-Krastanow growth mode.^{25–27} The islands began forming after the deposition of approximately 1.6 monolayers (ML) of InAs; a total of 2.3–2.6 ML was deposited. The quantum dots were then capped with a 100 nm layer of GaAs. Structural characterization of the dots via atomic force microscopy (AFM) was performed on uncapped samples. These results yielded average dimensions of 8 nm and 15 nm for the dot height and lateral extent, respectively, and a density of $\sim 5 \times 10^{10}$ dots/cm². The observed structural dimensions are much smaller than the Bohr radius of the exciton in bulk InAs (~ 36.8 nm),²⁸ putting these quantum dots in the limit of strong confinement. In addition, the AFM images reveal a structural elongation of the quantum dots along the [110] crystal axis, similar to what has been widely reported for a number of quantum dot systems,^{11,13,29} including $\text{In}_x\text{Ga}_{1-x}\text{As}$ self-assembled quantum dot samples.^{30,31}

After growth the samples were subjected to rapid thermal annealing at 750 °C for 30 sec to shift the exciton transitions to higher energies,^{32–36} to be accessible to available laser systems. To allow for the optical measurements to be performed in transmission, the sample was mounted to a *c*-axis normal sapphire disk, and the GaAs substrate was removed using a liquid chemical etch. The sample was mounted into a continuous flow liquid helium cryostat and held at a temperature of 7 K.

The structural asymmetry observed in quantum dots is found to greatly impact the optical properties of the excitons and biexcitons confined within these structures. In bulk and some quantum well samples, there exists translational symmetry within the plane of the structure. In such cases, the exciton states, such as the heavy hole states $| -1/2, +3/2 \rangle$ and $| +1/2, -3/2 \rangle$, are excited by circularly polarized light. A biexciton state consists of a combination of these two states, and can therefore be excited by two circularly polarized pho-

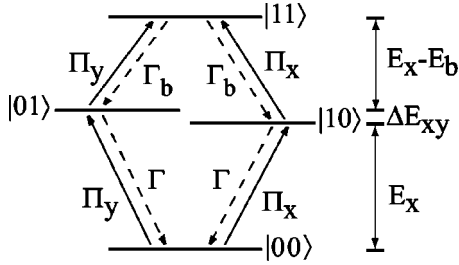


FIG. 1. Energy-level diagram for the exciton and biexciton transitions in a structurally elongated quantum dot. The states are labeled in the two exciton basis, with $|00\rangle$, $|10\rangle$, $|01\rangle$, and $|11\rangle$ corresponding to the ground, exciton, and biexciton states, respectively. Both the polarization selection rules for the optical transitions and the population decay paths are also indicated.

tons, of opposite helicity. In the elongated quantum dots, however, the symmetry is broken; this leads to a mixing of the exciton spin doublet via the exchange interaction, resulting in two linearly polarized transitions which are aligned along the orthogonal in-plane axes of the dot structure.^{11,13,29,30,37}

Figure 1 shows the energy level diagram for such a structure. Here we have labeled the states in the two exciton basis: $|00\rangle$ corresponds to the crystal ground state (no excitation); $|10\rangle$ and $|01\rangle$ are the single exciton states excited by Π_x - and Π_y -polarized light, respectively; and $|11\rangle$ corresponds to the biexciton state. The associated biexciton binding energy is denoted as ΔE_b . Note that unlike the case of higher-dimensional semiconductors, where photons of opposite polarization are required to excite the biexciton, here two parallel, linearly polarized photons are required.^{11,13,18,38} Also indicated are the population relaxation pathways, between the biexciton and exciton states (Γ_b), and the exciton and ground states (Γ). We have ignored spin-flip related relaxation between the single exciton states, based on our previously reported results showing these processes are strongly suppressed in this sample.⁸ In addition, those results showed that at zero magnetic field the exciton polarization states are slightly nondegenerate, with a typical energy splitting ΔE_{xy} of $\sim 40 \mu\text{eV}$.

II. EXPERIMENTAL METHODS

The measurements are performed using two pulsed optical fields $\mathbf{E}_1(\omega_1, t)$ and $\mathbf{E}_2(\omega_2, t - \tau)$ each having its respective polarization. The temporal delay between the two fields is designated by τ . These fields interact with the sample to produce a nonlinear polarization, which in turn radiates a signal field along the direction of the probe field \mathbf{E}_2 . Both of these fields are then homodyne-detected on a square-law detector. The nonlinear polarization is calculated to third order in the applied fields, and will in general contain contributions from several different perturbation sequences. In the spectral hole burning experiments, both frequency and polarization can be used to determine which of these will actually be present. For the discussion presented here, we will assume that the first field \mathbf{E}_1 always has polarization Π_y corresponding to excitation of the $|01\rangle$ exciton transition. The polariza-

tion, energy detuning, and temporal delay of the probe pulse with respect to the pump pulse can all be adjusted, in order to control which of the transitions shown in Fig. 1 will contribute to the nonlinear response. The expected results for such measurements can be understood using the density-matrix formalism.³⁹ There are several possible perturbation sequences to third order in the applied fields, which can give rise to a nonlinear signal in the DT geometry.

For those cases in which the energy of \mathbf{E}_2 is tuned around that of \mathbf{E}_1 , so that the exciton transition is probed, there are the pathways

$$\rho_{00,00} \xrightarrow{\mathbf{E}_1} \rho_{00,01} \xrightarrow{\mathbf{E}_1^*} \left\{ \begin{array}{l} \rho_{00,00} \\ \rho_{01,01} \end{array} \right\} \xrightarrow{\mathbf{E}_2 \parallel \mathbf{E}_1} \rho_{00,01}, \quad (1)$$

$$\rho_{00,00} \xrightarrow{\mathbf{E}_1} \rho_{00,01} \xrightarrow{\mathbf{E}_1^*} \left\{ \begin{array}{l} \rho_{00,00} \\ \rho_{01,01} \end{array} \right\} \xrightarrow{\mathbf{E}_2 \perp \mathbf{E}_1} \rho_{00,10}. \quad (2)$$

Both pathways result in induced transmission at the exciton energy, i.e., spectral hole burning, although in the second pathway, where \mathbf{E}_2 is polarized orthogonal to \mathbf{E}_1 , the signal will arise solely from the depletion of the ground-state population. In spectral hole burning measurements made with very narrow bandwidth lasers, the linewidth of the spectral hole is related to the dephasing rate of the transition. However, in the case of pulsed measurements such as these, in which the pulse width is much shorter than the dephasing time, the spectral hole will be determined by the spectrum of the optical pulses.

For excitation of the biexciton transition, in which the probe is detuned from the pump energy by an amount equal to the biexciton binding energy, there is no signal in case of orthogonally polarized pulses (in the absence of spin relaxation). For the parallel polarized case, two possible pathways exist

$$\rho_{00,00} \xrightarrow{\mathbf{E}_i} \rho_{00,01} \xrightarrow{\mathbf{E}_j^*} \left\{ \begin{array}{l} \rho_{00,00} \\ \rho_{01,01} \end{array} \right\} \xrightarrow{\mathbf{E}_k} \rho_{11,01}, \quad (3)$$

$$\rho_{00,00} \xrightarrow{\mathbf{E}_i} \rho_{00,01} \xrightarrow{\mathbf{E}_j^*} \rho_{00,11} \xrightarrow{\mathbf{E}_k} \rho_{00,01}. \quad (4)$$

The first of these corresponds to the stepwise excitation of the biexciton, with $\mathbf{E}_i = \mathbf{E}_j = \mathbf{E}_1$ and $\mathbf{E}_k = \mathbf{E}_2$. In this case, real exciton population is created, which is then driven to the biexciton state. This results in induced absorption of the probe at the exciton to biexciton transition, leading to an antihole. The final sequence corresponds to the two-photon coherence pathway. In this case, a coherence between the ground and biexciton states is first created, rather than a real exciton population. This contribution has been observed in frequency-domain measurements of single quantum dots,¹⁸ however, in the present measurements which utilize pulsed sources, this term could only contribute if either one of two conditions were met (while assuming that time ordering in the pump-probe geometry must be maintained, i.e., \mathbf{E}_2 does not arrive before \mathbf{E}_1 , and local field corrections are ignored). First, if the spectral bandwidth of the pulses was sufficiently

large relative to the biexciton binding energy, such that either pulse could excite both the exciton and biexciton transitions, then the term can contribute, even with a temporal delay between the pulses, with $\mathbf{E}_i = \mathbf{E}_j = \mathbf{E}_1$ and $\mathbf{E}_k = \mathbf{E}_2$. Otherwise, if the bandwidths are much smaller than the binding energy then the pulses must be overlapped in time, such that $\mathbf{E}_i = \mathbf{E}_k = \mathbf{E}_1$ and $\mathbf{E}_j = \mathbf{E}_2$. In our experiments the first condition is not met, as will be observed in the results. Likewise, as all of the results shown are obtained with a small positive temporal delay between the pump and probe pulses, the second condition is not met. Therefore we will not consider contributions from the two-photon coherence in discussing the data.

For these experiments, both of the fields \mathbf{E}_1 and \mathbf{E}_2 were obtained from a single mode locked Ti:sapphire laser, operating at a repetition rate of 76 MHz. The output pulses had a spectral bandwidth of approximately 16 meV (full width at half maximum—FWHM). The laser output was split into separate paths for the pump and probe fields. In order to have the two fields at different and independently tunable frequencies ω_1 and ω_2 , two pulse shapers were used.⁴⁰ The pulse shapers each consisted of a grating and lens pair, which imaged the spectrum of the pulses on a variable slit assembly, which acts as a spectral amplitude filter. By adjusting the width and horizontal position of the slits, the bandwidth and center frequency of the shaped pulse could be controlled. For these measurements, the shaped pulses had a spectral bandwidth of ~ 1.4 meV (FWHM). Optical cross-correlation measurements, utilizing an unshaped reference pulse, yielded a temporal duration of approximately 2.8 psec. In the case of the probe field \mathbf{E}_2 , the position of slit assembly was scanned using a computer-controlled stepping motor, to allow for averaging of spectral scans. A motorized linear translation stage controlled the temporal delay between the two fields.

Amplitude modulation at frequencies near 1 MHz was used, via traveling-wave acousto-optic modulators. The two arms of the experiment differed in modulation frequency by an amount δ . The signal and probe fields were homodyne detected on a silicon photodiode, and the resulting DT signal was measured using lock-in detection at this difference frequency δ . In order to improve the signal-to-noise ratio in the measurement, balanced detection was utilized, using a second photodiode and a reference field which did not pass through the sample. In addition, because the peak power changes as the spectral position was varied, a separate scan, without the pump field \mathbf{E}_1 present, was made to measure the transmission (T) of the probe field. The data shown in this paper are plotted as the normalized nonlinear response DT/T.

III. RESULTS AND DISCUSSION

Figure 2 shows the low-temperature PL and nonlinear DT spectra of the quantum dot ensemble, in the upper and lower traces, respectively. The PL spectrum is obtained with continuous-wave excitation at 2.5 eV, well above the energy bandgap of the GaAs barrier layers. The PL peak is centered at 1.287 eV, with an inhomogeneous linewidth of ~ 37.5 meV (FWHM). As has been widely reported for similar quantum dot samples,^{33,36,41–46} at higher excitation inten-

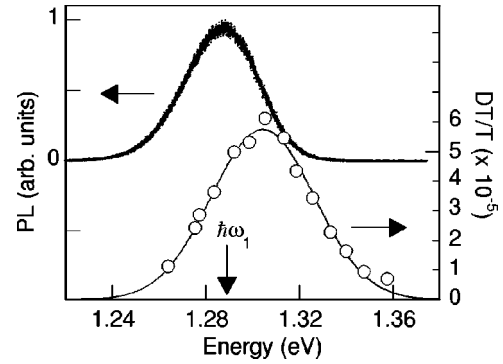


FIG. 2. Low-temperature PL (upper trace) and degenerate DT (lower trace) spectra of the InAs quantum dot ensemble. The PL, obtained under nonresonant excitation at 2.5 eV is peaked at 1.287 eV, with an inhomogeneous linewidth of 37.5 meV (FWHM). The DT spectrum is obtained by tuning the energy of the degenerate pump and probe pulses, with the temporal delay fixed at +2 psec. The solid line is a fit to a Gaussian function, peaked at 1.304 eV with a FWHM of 51.94 ± 1.32 meV. A shift of ~ 17 meV between the peaks of the PL and nonlinear spectra is observed. Figures are offset for clarity. The arrow indicates the spectral position of the pump field for the spectral hole burning measurements.

sities, emission from the higher-energy excited state is observed, with a ground-excited state splitting of approximately 50 meV in this sample.⁴⁷ The degenerate DT spectrum was measured by fixing the pump-probe temporal delay to +2 psec, and tuning the degenerate ($\omega_1 = \omega_2$) excitation fields. The data are indicated by the filled circles, while the solid line is a fit to a Gaussian function, centered at 1.304 eV, with a linewidth of 51.94 ± 1.32 meV (FWHM). While the observed energy shift of 17 meV with respect to the PL is large compared to that observed in higher-dimensional semiconductors, it is still much smaller than the excited state splitting in this sample. Both spectra show the quantum dot ensemble to be strongly inhomogeneously broadened; by comparison, recent four-wave-mixing measurements have inferred homogeneous linewidths which are orders of magnitude smaller, at only a few micro electron volt.^{9,10}

We now turn to the case of spectral hole burning, in which the two fields are nondegenerate ($\omega_1 \neq \omega_2$). The pump field \mathbf{E}_1 is tuned to 1.288 eV, on the low-energy side of the nonlinear response observed, as indicated by the arrow in Fig. 2; the pump spectrum is shown for reference in Fig. 3(a). First, we consider the case of the two fields having orthogonal, linear polarizations, corresponding to pathway (2) in the density-matrix picture previously discussed. In this polarization configuration, the signal results from the depletion of the ground-state exciton population, and does not have any contribution from the biexciton. These data are shown in Fig. 3(b), where the nonlinear signal is plotted as a function of the energy shift from the pump [$\hbar(\omega_2 - \omega_1)$], for a fixed temporal delay of +6 psec. As expected, the nonlinear response is peaked at the pump energy position; the data are well fitted by a Gaussian function (indicated by the solid line). The width of the spectral hole obtained from the fitting is 1.44 ± 0.04 meV (FWHM), which is significantly narrower

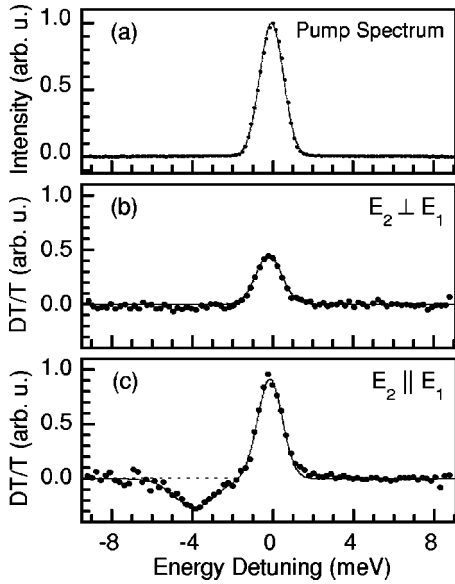


FIG. 3. Polarization dependent spectral hole burning measured in the InAs quantum dot ensemble, plotted as a function of energy detuning from the center of the pump spectrum: (a) spectrum of the pump pulse, where zero detuning corresponds to 1.288 eV. (b) spectral hole burning, at a temporal pump-probe delay of +6 psec, observed when the two excitation fields have orthogonal, linear polarizations. The spectral hole linewidth of 1.44 ± 0.04 meV corresponds to the bandwidth of the optical pulses and not the true homogeneous linewidth of the quantum dot transitions. (c) as (b), but for parallel linear field polarizations. In addition to the saturation response at zero detuning, an induced absorption resonance is observed at lower energy, indicating absorption on the exciton-biexciton transition. A binding energy of 3.75 ± 0.07 meV for the biexciton is obtained from the fitting.

than the observed inhomogeneous linewidth of the ensemble, and corresponds to the bandwidth of the optical pulses. The shape and width of the spectral hole is in agreement with our hypothesis that the homogeneous linewidth of these quantum dots is much narrower than our optical pulse bandwidth.

We now turn to the case of parallel, linearly polarized excitation fields, which corresponds to excitation pathway (1). In this case, if the probe field \mathbf{E}_2 is tuned to the wavelength of the pump field \mathbf{E}_1 , the response due to bleaching of the exciton absorption will be observed. If however, it is instead detuned by an amount equal to the binding energy of the biexciton state, an induced absorption resonance should be present, corresponding to the stepwise excitation of the biexciton as in pathway (3). Figure 3(c) shows the data obtained for this polarization configuration. At zero detuning, corresponding to the exciton response, a peak is observed. The magnitude of this signal is twice that of the orthogonal polarization case in Fig. 3(b), due to the contribution of both saturation and ground-state depletion. The spectral width is, within the accuracy of the fitting, the same as in (b), as one would expect. At energies below the pump position, a clear induced absorption response is observed, corresponding to absorption to the biexciton state. While biexciton states in self-assembled dots have been previously studied using PL spectroscopy,^{15–17} this represents the first evidence of the

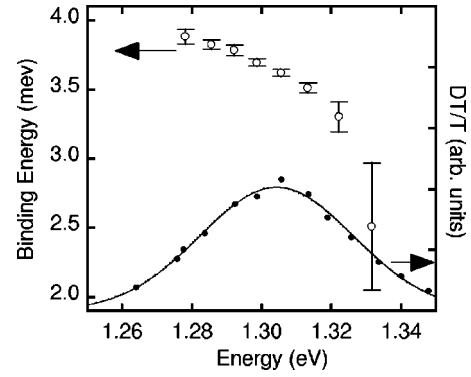


FIG. 4. Dependence of the biexciton binding energy (open circles) on the energy tuning of the pump pulse within the inhomogeneous distribution. The degenerate DT spectrum is shown as a reference.

biexciton state in nonlinear spectroscopy in these systems.

Fitting the data to a combination of two Gaussian functions (indicated by the solid line), we obtain a biexciton binding energy of 3.75 ± 0.07 meV. As expected for confined structures, this binding energy is much larger than those observed in GaAs bulk⁴⁸ or quantum well⁴⁹ samples, and is comparable to that reported in single dot PL for InAs-based quantum dots.^{15–17} The fitted width of the biexciton response, 2.393 ± 0.17 meV, is slightly wider than the exciton peak. We attribute this observation to the ensemble nature of the measurements: excitons which have similar transition energies, and thus are excited by the pump pulse, may have different biexciton binding energies, resulting in a larger width for the induced absorption response.

The binding energy of the biexciton state is found to vary across the inhomogeneous ensemble of quantum dots, obtained by measuring the spectral hole burning response as a function of the pump position within the inhomogeneously broadened nonlinear response. These results are shown in Fig. 4, where the measured biexciton binding energies (open circles) are plotted as a function of the pump field \mathbf{E}_1 energy, corresponding to a subset of exciton transition energies. For reference, the degenerate DT spectrum (from Fig. 2) is shown as well. At the lowest energy which could be attained with our experimental setup, 1.278 eV, a binding energy of ~ 3.9 meV was measured. However, as the energy of the pump field \mathbf{E}_1 is increased, the binding energy decreases by almost a factor of two, down to ~ 2.5 meV at the highest energy studied, 1.332 eV.

The inhomogeneous spectrum of the quantum dot ensemble reflects variations in the physical properties of the dots, e.g., size, strain, shape, or indium content; these parameters will also strongly influence the biexciton binding energy.^{50,51} For self-assembled structures, previous results have shown that increasing exciton recombination energies can be correlated with decreasing dot size^{15,42,52,53} and decreasing indium concentration.^{54,55} The exact structure and composition of the present samples after annealing is not known, and both of these effects likely impact the observed results. In both cases, the electron and hole states in those dots with higher exciton recombination energies are less

strongly localized than those at lower energies, resulting in a decrease in the electron-hole wave-function overlap. The Coulomb repulsion between like particles can then begin to offset, and eventually dominate, the electron-hole attraction. The net result is a decrease in biexciton binding energy as the exciton recombination energy is increased,^{50,51,56,57} as observed in Fig. 4. We note that similar trends in the biexciton binding energy have been observed in single quantum dot emission studies,⁵⁸ as have the negative binding energy antibound states.^{58,59} These previous observations, as well as our own, are in contrast to results from larger quantum dot structures, in which the size of the dot is comparable to or somewhat larger than the exciton bulk Bohr radius. In that case, there is an enhancement of the Coulomb interaction between the excitons due to the increased wave-function overlap caused by confinement. As the size of the quantum dot is decreased, the biexciton binding energy is increased, as observed experimentally for several systems, including II-VI nanocrystals^{60,61} and larger $\text{In}_x\text{Ga}_{1-x}\text{As}$ dots.¹⁵

IV. CONCLUSIONS

In this paper we have reported on polarization-dependent spectral hole burning measurements in an ensemble of InAs

quantum dots, in which we have directly observed the induced absorption resulting from the quantum dot biexcitons. As a result of the confinement enhancement, a large binding energy of 3.75 ± 0.07 meV is measured. The binding energy shows a strong dependence on the size of the quantum dots, varying by nearly a factor of two over the inhomogeneous distribution of dots. These measurements will hopefully lead to further studies of biexcitons in these strongly confined structures, such as the measurement of the two-photon coherent excitation, similar to that observed in GaAs quantum dots.¹⁸

ACKNOWLEDGMENTS

This work was supported in part by the U.S. Army Research Office under Contract/Grant No. DAAD19-99-1-0198, by the National Security Agency and Advanced Research and Development Activity under Army Research Office Contract No. DAAG55-98-1-0373, by the Air Force Office of Scientific Research under Grant No. F49620-99-1-0045, and by the National Science Foundation through the Center for Ultrafast Optical Science at the University of Michigan under Grant No. STC-PHY-8920108.

*Present address: The Laboratory for Physical Sciences, College Park, MD 20740.

†Electronic address: dst@umich.edu

¹E. Biolatti, R.C. Iotti, P. Zanardi, and F. Rossi, *Phys. Rev. Lett.* **85**, 5647 (2000).

²P. Chen, C. Piermarocchi, and L.J. Sham, *Phys. Rev. Lett.* **87**, 067401 (2001).

³T.H. Stievater, X. Li, D.G. Steel, D. Gammon, D.S. Katzer, D. Park, C. Piermarocchi, and L.J. Sham, *Phys. Rev. Lett.* **87**, 133603 (2001).

⁴H. Kamada, H. Gotoh, J. Temmyo, T. Takagahara, and H. Ando, *Phys. Rev. Lett.* **87**, 246401 (2001).

⁵H. Htoon, T. Takagahara, D. Kulik, O. Baklenov, A.L. Holmes, Jr., and C.K. Shih, *Phys. Rev. Lett.* **88**, 087401 (2002).

⁶A. Zrenner, E. Beham, S. Stufler, F. Findeis, M. Bichler, and G. Abstreiter, *Nature (London)* **418**, 612 (2002).

⁷G. Chen, N.H. Bonadeo, D.G. Steel, D. Gammon, D.S. Katzer, D. Park, and L.J. Sham, *Science* **289**, 1906 (2000).

⁸A.S. Lenihan, M.V.G. Dutt, D.G. Steel, S. Ghosh, and P.K. Bhattacharya, *Phys. Rev. Lett.* **88**, 223601 (2002).

⁹P. Borri, W. Langbein, S. Schneider, U. Woggon, R.L. Sellin, D. Ouyang, and D. Bimberg, *Phys. Rev. Lett.* **87**, 157401 (2001).

¹⁰D. Birkedal, K. Leosson, and J.M. Hvam, *Phys. Rev. Lett.* **87**, 227401 (2001).

¹¹V.D. Kulakovskii, G. Bacher, R. Weigand, T. Kummell, A. Forchel, E. Borovitskaya, K. Leonardi, and D. Hommel, *Phys. Rev. Lett.* **82**, 1780 (1999).

¹²K. Brunner, G. Abstreiter, G. Böhm, G. Tränkle, and G. Weimann, *Phys. Rev. Lett.* **73**, 1138 (1994).

¹³L. Besombes, K. Kheng, and D. Martrou, *Phys. Rev. Lett.* **85**, 425 (2000).

¹⁴Q. Wu, R.D. Grober, D. Gammon, and D.S. Katzer, *Phys. Rev. B* **62**, 13 022 (2000).

¹⁵M. Bayer, T. Gutbrod, A. Forchel, V.D. Kulakovskii, A. Gorbunov, M. Michel, R. Steffen, and K.H. Wang, *Phys. Rev. B* **58**, 4740 (1998).

¹⁶A. Kuther, M. Bayer, A. Forchel, A. Gorbunov, V.B. Timofeev, F. Schäfer, and J.P. Reithmaier, *Phys. Rev. B* **58**, R7508 (1998).

¹⁷H. Kamada, H. Ando, J. Temmyo, and T. Tamamura, *Phys. Rev. B* **58**, 16 243 (1998).

¹⁸G. Chen, T.H. Stievater, E.T. Batteh, X. Li, D.G. Steel, D. Gammon, D.S. Katzer, D. Park, and L.J. Sham, *Phys. Rev. Lett.* **88**, 117901 (2002).

¹⁹J. Shah, *Ultrafast Spectroscopy of Semiconductors and Semiconductor Nanostructures*, 1st ed. (Springer, Berlin, 1996).

²⁰Y. Sugiyama, Y. Nakata, S. Muto, T. Futatsugi, and N. Yokoyama, *IEEE J. Sel. Top. Quantum Electron.* **4**, 880 (1998).

²¹Y. Sugiyama, Y. Nakata, S. Muto, Y. Awano, and N. Yokoyama, *Physica E (Amsterdam)* **7**, 503 (2000).

²²T.S. Sosnowski, T.B. Norris, H. Jiang, J. Singh, K. Kamath, and P. Bhattacharya, *Phys. Rev. B* **57**, R9423 (1998).

²³J. Urayama, T.B. Norris, J. Singh, and P. Bhattacharya, *Phys. Rev. Lett.* **86**, 4930 (2001).

²⁴J. Feldmann, S.T. Cundiff, M. Arzberger, G. Böhm, and G. Abstreiter, *J. Appl. Phys.* **89**, 1180 (2001).

²⁵P. Berger, K. Chang, P. Bhattacharya, J. Singh, and K.K. Bajaj, *Appl. Phys. Lett.* **53**, 684 (1988).

²⁶D.J. Eaglesham and M. Cerullo, *Phys. Rev. Lett.* **64**, 1943 (1990).

²⁷D. Leonard, M. Krishnamurthy, C.M. Reaves, S.P. Denbaars, and P.M. Petroff, *Appl. Phys. Lett.* **63**, 3203 (1993).

²⁸H. Fu, L.-W. Wang, and A. Zunger, *Phys. Rev. B* **59**, 5568 (1999).

²⁹D. Gammon, E.S. Snow, B.V. Shanabrook, D.S. Katzer, and D. Park, *Phys. Rev. Lett.* **76**, 3005 (1996).

³⁰M. Bayer, A. Kuther, A. Forchel, A. Gorbunov, V.B. Timofeev, F. Schäfer, J.P. Reithmaier, T.L. Reinecke, and S.N. Walck, *Phys. Rev. Lett.* **82**, 1748 (1999).

- ³¹M. Bayer, A. Kuther, A. Forchel, and T.L. Reinecke, *Phys. Status Solidi A* **178**, 297 (2000).
- ³²A.O. Kosogov, P. Werner, U. Gösele, N.N. Ledentsov, D. Bimberg, V.M. Ustinov, A.Y. Egorov, A.E. Zhukov, P.S. Kop'ev, N.A. Bert, and Z.I. Alferov, *Appl. Phys. Lett.* **69**, 3072 (1996).
- ³³S. Malik, C. Roberts, R. Murray, and M. Pate, *Appl. Phys. Lett.* **71**, 1987 (1997).
- ³⁴S.J. Xu, X.C. Wang, S.J. Chua, C.H. Wang, W.J. Fan, J. Jiang, and X.G. Xie, *Appl. Phys. Lett.* **72**, 3335 (1998).
- ³⁵B. Lita, R.S. Goldman, J.D. Phillips, and P.K. Bhattacharya, *Appl. Phys. Lett.* **75**, 2797 (1999).
- ³⁶T.M. Hsu, Y.S. Lan, W.-H. Chang, N.T. Yeh, and J.-I. Chyi, *Appl. Phys. Lett.* **76**, 691 (2000).
- ³⁷T. Takagahara, *Phys. Rev. B* **62**, 16 840 (2000).
- ³⁸T.H. Stievater, X. Li, D.G. Steel, D. Gammon, D.S. Katzer, and D. Park, *Phys. Rev. B* **65**, 205319 (2002).
- ³⁹Discussions of the density-matrix formalism can be found in, for example, I.M. Beterov and V.P. Chebotaev, *Prog. Quantum Electron.* **3**, 1 (1974); or M. O. Scully and M. S. Zubairy, *Quantum Optics* (Cambridge University Press, Cambridge, 1997).
- ⁴⁰For a review of pulse-shaping techniques, see A.M. Weiner, *Prog. Quantum Electron.* **19**, 161 (1995), and references therein.
- ⁴¹S. Raymond, S. Fafard, P.J. Poole, A. Wojs, P. Hawrylak, S. Charbonneau, D. Leonard, R. Leon, P.M. Petroff, and J.L. Merz, *Phys. Rev. B* **54**, 11 548 (1996).
- ⁴²K.H. Schmidt, G. Medeiros-Ribeiro, M. Oestreich, P.M. Petroff, and G.H. Döhler, *Phys. Rev. B* **54**, 11 346 (1996).
- ⁴³R. Heitz, M. Veit, N.N. Ledentsov, A. Hoffmann, D. Bimberg, V.M. Ustinov, P.S. Kop'ev, and Z.I. Alferov, *Phys. Rev. B* **56**, 10 435 (1997).
- ⁴⁴K. Kamath, N. Chervela, K.K. Linder, T. Sosnowski, H.-T. Jiang, T. Norris, J. Singh, and P. Bhattacharya, *Appl. Phys. Lett.* **71**, 927 (1997).
- ⁴⁵I.E. Itskevich, M.S. Skolnick, D.J. Mowbray, I.A. Trojan, S.G. Lyapin, L.R. Wilson, M.J. Steer, M. Hopkinson, L. Eaves, and P.C. Main, *Phys. Rev. B* **60**, R2185 (1999).
- ⁴⁶D. Morris, N. Perret, and S. Fafard, *Appl. Phys. Lett.* **75**, 3593 (1999).
- ⁴⁷A. S. Lenihan and D. G. Steel (unpublished).
- ⁴⁸G.W. 't Hooft, W.A.J.A. van der Poel, L.W. Molenkamp, and C.T. Foxen, *Phys. Rev. B* **35**, 8281 (1987).
- ⁴⁹R.C. Miller, D.A. Kleinman, A.C. Gossard, and O. Munteanu, *Phys. Rev. B* **25**, 6545 (1982).
- ⁵⁰O. Stier, A. Schliwa, R. Heitz, M. Grundmann, and D. Bimberg, *Phys. Status Solidi B* **224**, 115 (2001).
- ⁵¹O. Stier, R. Heitz, A. Schliwa, and D. Bimberg, *Phys. Status Solidi A* **190**, 477 (2002).
- ⁵²M. Grundmann, O. Stier, and D. Bimberg, *Phys. Rev. B* **52**, 11 969 (1995).
- ⁵³A. Endoh, Y. Nakata, Y. Sugiyama, M. Takatsu, and N. Yokoyama, *Jpn. J. Appl. Phys.* **38**, 1085 (1999).
- ⁵⁴W. Sheng and J.-P. Leburton, *Phys. Rev. B* **63**, 161301 (2001).
- ⁵⁵J. Shumway, A.J. Williamson, A. Zunger, A. Passaseo, M. DeGiorgi, R. Cingolani, M. Catalano, and P. Crozier, *Phys. Rev. B* **64**, 125302 (2001).
- ⁵⁶T. Takagahara, *Phys. Rev. B* **39**, 10 206 (1989).
- ⁵⁷T. Tsuchiya, *Physica E (Amsterdam)* **7**, 470 (2000).
- ⁵⁸S. Rodt, R. Heitz, A. Schliwa, R.L. Sellin, F. Guffarth, and D. Bimberg, *Phys. Rev. B* **68**, 035331 (2003).
- ⁵⁹L. Landin, M.S. Miller, M.-E. Pistol, C.E. Pryor, and L. Samuelson, *Science* **280**, 262 (1998).
- ⁶⁰Y.Z. Hu, S.W. Koch, M. Lindberg, N. Peyghambarian, E.L. Pollock, and F.F. Abraham, *Phys. Rev. Lett.* **64**, 1805 (1990).
- ⁶¹K.I. Kang, A.D. Kepner, S.V. Gaponenko, S.W. Koch, Y.Z. Hu, and N. Peyghambarian, *Phys. Rev. B* **48**, 15 449 (1993).